



HHS Public Access

Author manuscript

J Biomed Mater Res B Appl Biomater. Author manuscript; available in PMC 2024 March 01.

Published in final edited form as:

J Biomed Mater Res B Appl Biomater. 2023 March ; 111(3): 599–609. doi:10.1002/jbm.b.35177.

In Vivo Biocompatibility of SrO and MgO Doped Brushite Cements

Samit K. Nandi^{1,*}, Mangal Roy^{2,}, Amit Bandyopadhyay^{2,*}, Susmita Bose^{2,*}**

¹Department of Veterinary Surgery and Radiology, West Bengal University of Animal and Fishery Sciences, Kolkata-700037, India.

²W. M. Keck Biomedical Materials Research Laboratory, School of Mechanical and Materials Engineering, Washington State University, Pullman, WA 99164-2920, USA.

Abstract

The addition of dopants in biomaterials has emerged as a critical regulator of bone formation and regeneration due to their imminent role in the biological process. The present work evaluated the role of strontium (Sr) and magnesium (Mg) dopants in brushite cement (BrC) on *in vivo* bone healing performance in a rabbit model. Pure, 1wt% SrO (Sr-BrC), 1wt% MgO (Mg-BrC), and a binary composition of 1.0 wt% SrO+1.0 wt% MgO (Sr+Mg-BrC) BrCs were implanted into critical-sized tibial defects in rabbits for up to 4 months. The *in vivo* bone healing of three doped and pure BrC samples was examined and compared using sequential radiological examination, histological evaluations, and fluorochrome labeling studies. The results indicated excellent osseous tissue formation for Sr-BrC and Sr+Mg-BrC and moderate bone regeneration for Mg-BrC compared to pure BrC. Our findings indicated that adding small amounts of SrO, MgO, and binary dopants to the BrC can significantly influence new bone formation for bone tissue engineering.

Keywords

Brushite cement; Bioceramics; Dopants; Bone disorders; Calcium phosphate

1.0 Introduction

Calcium phosphates (CaP)-based bone substitutes are frequently used due to their strong bone-material interface and excellent biocompatibility *in vivo* [1,2]. Among the various CaPs, the cement form has emerged as a candidate for bone graft substitutes, specifically treating small-scale bone defects, vehicles for drug delivery, and stabilizing load-bearing implants [2]. CaP cement's specific properties, such as chemical composition similar to bone, low setting temperature, and easy deformability at the application site, are essential for bone substitutes [1–4]. Among the two forms of calcium phosphate cement, apatite and

*Corresponding authors - sbose@wsu.edu; Dr. Samit K. Nandi: drsknandi@wbuafl.ac.in.

**Current affiliation – Metallurgical and Materials Engineering, IIT-Kharagpur, India.

Conflict of Interest

None.

brushite, brushite cement (BrC) has gained significant interest due to its higher *in vivo* resorbability and concerns related to the metastable CaP phase in physiological conditions of apatite cement [2, 5–7]. Brushite is dicalcium phosphate dihydrate (DCPD, $\text{CaHPO}_4 \cdot 2\text{H}_2\text{O}$), a crystalline form of CaPs. Typically, a local decrease in pH and quick setting properties are concerns for BrC [8]. Several modifiers have been used to modulate the setting time of BrC, including sodium hydrogen phosphate, compounds of sulfate and citrate, and the addition of various metal ions [2,9–11].

Bone accepts BrC, soft tissue environment *in vivo*, and cement resorption intimately pursued by new bone formation. However, the new generation of resorbable biomaterials is predicted to be osteoinductive, inducing new bone formation [12]. The most common procedure to enhance biological performance vis-à-vis osseointegration in CaP cement is to incorporate bone-derived growth factors such as bone morphogenetic protein (BMP), insulin-like growth factor (IGF), vascular endothelial growth factor (VEGF), transforming growth factor β (TGF- β) that trigger bone regeneration [13,14]. Nevertheless, the long-term viability of the protein in the material is a significant challenge. Several approaches have been tried to improve osteoconductivity or induce osteoinductivity of BrC to overcome these challenges and concerns with stability/storage of growth factors and proteins, including modifying the composition of BrC, stem cell seeding, etc. These modifications in BrC can achieve better osteoinductivity and osteostimulation in the bone regeneration process and enhance physicochemical properties [15–17].

In recent years ionic substitutions in CaP cement have been the topic of great interest due to their critical role in overall bone turnover. Among different metal ions, strontium (Sr), zinc (Zn), and magnesium (Mg) are the predominant [2,7,9–11,15,18–20]. The co-substitution of Sr and Zn in BrC has been observed to reduce the setting time while improving compressive strength, pre-osteoblast proliferation, and osteoblast maturation [9,10]. Similarly, Mg substitution in BrC could improve mechanical properties and enhance osteoblast cell proliferation and differentiation [11]. Mg plays a significant role in the enhanced bone calcification process and indirectly influences bone weakness and mineral metabolism [21–23]. Moreover, Mg deficiency in bone has been considered a potential risk factor for osteoporosis in humans [24–27]. Similarly, Sr, a critical metal ion, has been extensively used with CaP cement to treat osteoporosis [7,10]. Strontium helps to prevent bone loss through its action on diminishing differentiation and resorbing activity of osteoclasts [28]. Additionally, Sr^{2+} enhances osteoclast apoptosis and increases pre-osteoblastic cell proliferation and collagen synthesis, decreasing bone resorption and preserving bone formation [29,30]. These results are based on high dopant concentrations, typically >5 wt%. A 5 wt% Sr^{2+} addition to BrC completely filled a bone defect in osteoporotic rabbits within 8 weeks [31]. Sr^{2+} addition to BrC also showed a significant increase in compressive strength, from ~ 1.0 MPa to >30 MPa [32]. However, during the past decade, the use of high Sr^{2+} ions has been restricted due to overestimation of bone growth, increasing blood clots among patients, and a higher number of heart attacks than patients who were not exposed to a high dose of Sr^{2+} ions [33]. Like Sr^{2+} ions, most Mg^{2+} studies are also done with a high dose in BrC to show improvements in injectability, compressive strengths [34, 35], and new bone formation [36]. Since limited

data are available on the influence of low-dose Sr^{2+} and Mg^{2+} ions addition to BrC, a knowledge gap exists, which is the focus of this study.

The present study's objectives are to evaluate low-dose Sr and Mg doping's influence on the *in vivo* bone formation and osseointegration capacity in a critical-sized bone defect in the animal model over two-time points of 2 and 4 months. We hypothesize that the rapidly dissolving doped BrC will release the metal ions, enhancing the osseointegration of BrC at the early stages of wound healing. Since many studies have already confirmed the influence of these dopants on the mechanical properties of BrC, our studies' focus remained only on *in vivo* biological responses. The *in vivo* osseointegration was characterized by sequential radiographs, fluorochrome labeling, and histology.

2.0 Materials and Methods

2.1 Cement preparation

The BrC was prepared by mixing β -tricalcium phosphate (β -TCP) and monocalcium phosphate monohydrate (MCPM, Sigma Aldrich, USA) [37]. The optimized cement formation process has been explained in our previous work [38]. Briefly, in-house prepared β -TCP powders were mixed with MCPM, magnesium hydrogen phosphate trihydrate, sodium hydrogen phosphate, and magnesium sulfate [5,39] to form the BrC. A powder-to-liquid ratio of 3.33:1 was used to achieve a workable consistency. Dopant was introduced during the synthesis of the β -TCP powder. The doped β -TCP powder was used to prepare the doped cement. In the present work, 1.0 wt% SrO (Sr-BrC) and 1.0 wt% MgO (Mg-BrC) and a binary composition of 1.0 wt% SrO+1.0 wt% MgO (Sr+Mg-BrC) were introduced in the cement.

2.2 Physico-mechanical properties

The Gillmore needle measured the cement's initial and final setting time following ASTM C266. The cement paste was poured into a split steel mold of 6 mm in diameter and 12 mm in height. This method placed a needle of 2.12 mm in diameter and 113.4g on the cement sample. The initial set time was recorded when the needle could not impact the cement paste's surface. Similarly, a needle of 1.06 mm in diameter and 453.6g was used to determine the final setting time.

After preparing the samples in the split mold, cylindrical samples were removed from the mold and kept in phosphate-buffered saline (PBS) at 37 °C for 1 day [37]. Samples were dried overnight at room temperature and crushed to powder for XRD analysis. Phase analysis of the cement was characterized by Siemens D500 Krystalloflex X-ray diffractometer using Cu K α radiation at 35 kV and 30 mA at room temperature equipped with a Ni-filter over the 2θ range between 10 and 40 degrees, at a step size of 0.02 degrees and a count time of 1.0 sec per step. For the microstructural study, some fractured samples were collected and imaged using a field emission scanning electron microscope (FESEM, FEI 200F, FEI, OR).

2.3 In vivo study

In vivo experiments were carried out according to specifications in the guidelines for Animal Experiments of the Institutional Animal Ethical Committee of the West Bengal University of Animal and Fishery Sciences, India (Approval # E. C. 765). Twenty-four New Zealand white male rabbits of either sex with an average 2–2.5 kg weight were utilized. The animals were acclimatized for 2 weeks before being used in the experiment and were maintained under identical environments, management and standard balanced diet, and drinking water ad libitum. All the animals underwent bilateral surgery with control β -TCP cement in one limb and Sr-BrC, Mg-BrC, and Sr+Mg-BrC cement in the other limb. Eight rabbits per doped cement composition were used for the experiment. In each group, 4 rabbits were sacrificed at 2 and 4 months to assess and compare the progressive healing potentialities.

Under standard aseptic conditions and sedation with xylazine hydrochloride (1 mg/kg body weight; Indian Immunologicals, India) and Ketamine hydrochloride (11 mg/kg body weight; Ketalar[®], Parke-Davis, India) in combination with local 2% lignocaine hydrochloride (Neon Laboratories, India), 2 cm longitudinal skin incision was made on the medial side of the tibia bone in both the limbs [40]. The implant sites ($0.8 \times 0.4 \text{ cm}^2$) were prepared using a micro-motor dental drill after exposing the cortical bone, followed by irrigation with sterile normal saline. After implanting the respective cement, the muscle, subcutaneous tissue, and skin were sutured in layers. All the animals received cefotaxime sodium (125 mg IM twice daily; Mapra India, India) and injectable meloxicam (0.2 mL once daily for 5 days; Intas Pharmaceuticals, India) as an analgesic with daily dressing changes for surgical wounds.

2.3.1 Radiological investigations: Postoperatively, radiographs were taken on days 0, 30, 60, 90, and 120 to outline the bone-material interface and estimate the extent of bonding using a 300 mA medical diagnostic X-ray machine (M.E. X-ray, India).

2.3.2 Histological analysis: Histological analysis was carried out at 2 and 4 months to check the cellular response of the host bone to the implants. Bone specimens from the adjacent bone at the side and the bottom of the original bone defect were collected, washed thoroughly with normal saline, and fixed in 10% formalin for 7 days. All samples of bone tissue were decalcified (Goodling and Stewart's fluid containing formic acid 15 mL, formalin 5 mL, and distilled water 80 mL solution), followed by fixation with 4% paraformaldehyde. Then the samples were embedded into paraffin wax, 4 μm sections were prepared and stained with hematoxylin and eosin (H&E).

2.3.3 Fluorochrome labeling: Fluorochrome (oxytetracycline dehydrate; Pfizer India, India), at a dose of 25 mg/kg body weight, was given 3 weeks before each sacrifice time point. Undecalcified ground sections were prepared from the implanted segments of the bone, and the sections were ground to 20 μm thickness using different grades of sandpaper. The undecalcified ground sections were observed under incidental ultraviolet light with an Orthoplan microscope (Excitation filter, BP- 400 range, Leitz, USA) for tetracycline labeling to determine the amount and source of newly formed bone.

3.0 Results

3.1 Physico-chemical properties

Our initial optimization work resulted in a P/L ratio of 3.33:1 with 1 w% sodium pyrophosphate considering a workable setting time. The setting times of BrC, Sr-BrC, Mg-BrC, and Sr+Mg-BrC are shown in Table 1. Sr's presence in the cement mixture decreases the setting time, while Mg increases the initial and final setting time. Fig. 1 shows the X-ray diffraction patterns of pure and doped BrC samples after 1 day of incubation in PBS. The peaks were identified as β -TCP (JCPDS # 09-0169) and DCPD (JCPDS # 09-0077). The cement was mainly composed of a large amount of β -TCP and DCPD. Impurity phases were not detected in the cement samples. The amount of brushite (DCPD) and β -TCP calculated based on the X-ray diffraction patterns are listed in Table 1. As can be seen, the addition of Sr increased the DCPD the most. FESEM micrographs of the fracture surfaces of the cement samples are shown in Fig. 2. The cement samples were characterized by large amounts of unreacted β -TCP particles and needle/plate-shaped DCPD crystals. Sr-BrC showed higher DCPD crystal formation than BrC, Mg-BrC, and Sr+Mg-BrC cement.

3.2 Radiological examinations

Fig. 3 shows the radiographs of cement implanted rabbit proximal tibia as a function of implantation time and cement composition. At 0 day, all samples' radiographic images showed rectangular defects with well-placed cement. At 2 months, all of the radiographs for the doped samples were characterized by the absence of this zone which was still visible for pure BrC. Initiation of the new bone formation was also evident for all 3 doped cement samples, however prominent for Sr-BrC and Sr+Mg-BrC. Over time, all of the cement samples showed a complete absence of radiolucent zones except in BrC samples, where a shadow of the radiolucent zone was still visible. The defect area's radiodensity in all samples was comparable with the host bone, indicating osseointegration of the cement with the host bone was well under process. The new bone formation at 4 months in the defect area was similar in all 4 samples. However, a difference in bony tissue organization at the defect site was observed for pure and doped cement samples. The doped samples could not differentiate the host and the new bone, indicating complete integration of the doped cement.

3.3 Histological observations

Fig. 4 shows the histological evaluation at the bone-implant interface at 2 months. As shown in Fig. 4a, BrC cement shows Haversian lamella with osteoid proliferation, especially in an orderly manner. The medullary portion of bone showed a fair amount of mononuclear cells, red blood cells (RBC), osteoblast, and a few fibroblastic cells. The canalicular space was invaded by blood vessels showing regeneration with abundant collateral circulation. Compared to BrC cement, Sr-BrC cement showed much fibroblastic proliferation, higher osteoblastic activity, and a moderately vascular medullary portion supplied by many fat cells. Mg-BrC cement samples were characterized by parenchymal architecture of bony lamellae, vascular medulla, and canalicular space packed by proliferating osteoblastic cells shown in Fig. 4c. Moreover, calcification around the bony trabecular masses, fibrovascular tissue presence, and RBC in the sinusoidal space were also evident for Mg-BrC cement samples. Fig. 4d shows the histological images of Sr+Mg-BrC cement with fibroblastic

proliferation around the lamellar part of the bone. For this sample, some bony canaliculi were invaded by blood vessels and encircled with a ping deposit (eosinophilic deposit).

Histological evaluations at 4 months for the doped and pure cement are shown in Fig. 5. Compared to 2 months, visibly higher vascularization was noticed for all the cement samples. However, a noticeable difference in vascularization was found for Sr+Mg-BrC cement compared to other samples, as shown in Fig. 5d. It has also been noticed that fibroblastic activity was transformed into osteoblastic activity for all 4 cement samples. However, higher osteoblastic activity was noticed in Sr+Mg-BrC cement samples. These images are further quantified by measuring the ratio of osteoblasts and Haversian canals for each composition after 2 months of implantation (Fig. 6a). This analysis shows a similar trend to the new and old bone formation ratio. The highest ratio of ~ 150 % is seen for the Sr+Mg-BrC composition. The other compositions show a ratio of ~ 66 % (Sr-BrC), ~ 73 % (Mg-BrC), and ~ 33 % for the control sample respectively. After 4 months of in vivo study, the scaffolds show complete maturation of the Haversian canals. The number of matured canals is counted for each composition and plotted in Fig. 6b. The maturation of Haversian canals in the presence of these scaffolds in the later time point indicates the potential of the tested compositions for various bone tissue engineering applications.

3.4 Fluorochrome labeling study

Fig. 7a shows the fluorochromic images with oxytetracycline labeling where golden yellow fluorescence depicted new bone formation, and dark sea green appearances indicated matured old bone. Microphotograph viewed under fluorescent light imparted a double tone golden yellow fluorescence in a narrow zone in the defect site, and the host bone evinced dark sea green homogenous color in 2 months for BrC implanted bone. Higher golden yellow fluorescence was observed for Sr-BrC, Mg-BrC, and Sr+Mg-BrC cement samples. ImageJ software (NIH, USA) is used to quantify the areas in terms of pixels. The ratio of new bone and total bone formation is shown in Fig. 7b. The ratio of new bone and old bone is shown in Fig. 7c. Similar quantification of bone formation has been reported before [41]. In general, the area coverage of the new bone formation, as evident by golden yellow fluorescence, increased for all samples at 4 months. The Sr+Mg-BrC cement implanted bone showed multiple regions of new bone formation compared to BrC and Mg-BrC samples indicating rapid bone regeneration. Sr-BrC samples also showed increased new bone formation with broad coverage. The control BrC shows ~ 45 % of new bone formation after 2 months on implantation, which further increases to ~ 56 % after 4 months. The osteogenic effects of Sr and Mg lead to the highest ~ 90 % new bone formation after 2 months for the Sr+Mg-BrC composition, which increases to ~ 95% after 4 months. The Sr-BrC and Mg-BrC show 65 % and 81 % new bone formation after 2 months. The quantification results after 4 months indicate that these two compositions show ~ 77 % and 84 % new bone formation, respectively. Fig. 7c shows the ratio of new bone formation to the old bone. The results corroborate well with the new bone: total bone ratio, and a similar trend is observed. The highest ~ 1368 % of new bone is seen in the Sr+Mg-BrC composition after 4 months. The control shows ~ 127 % of new bone after 4 months compared to the old bone.

4.0 Discussion

BrC has gained considerable interest in stabilizing bone fractures and reinforcing osteoporotic bone [2,8]. Many approaches have been developed to improve further the bone integration of BrC, among which the addition of metal ion dopants is of significant interest. This study reports a simple processing technique for preparing low-dose Sr and Mg-doped BrC and *in vivo* biological responses in a rabbit model.

The setting of BrC locally decreases the pH value, leading to the cement's fibrous encapsulation and subsequent rejection by the body [6]. Excess β -TCP prevents the local release of H^+ ions from cement reaction and neutralizes the local pH decrease at an early stage of cement augmentation [42,43]. It has also been reported that the presence of β -TCP granules promotes mature bone formation [5]. In this work, excess β -TCP in the set cement results in good bone growth in all the cement samples without fibrous encapsulation. Granular β -TCP can be seen throughout the needle/plate-shaped DCPD phase. The setting reaction of BrC is influenced by metal ion dopants [7]. Although not very extensive, Sr's presence in the cement mixture decreases the setting time, while Mg increases the initial and final setting time.

The radiological investigation is ideal for characterizing *in vivo* orthopedic biomaterials to assess the union at host bone-material interfaces during follow-ups [44]. Sequential radiographic images are noninvasive characterization and allow to study of the nature and dynamics of the bone formation process and osseointegration of a resorbable biomaterial [45]. A discrete radiolucent zone at the bone-material interface is generally seen on the immediate postoperative radiographs. This zone's gradual absence is considered a signal of union between the implant and the host bone [46]. In the present study, the radiographic images in all the samples at 0 day show rectangular defects indicating the near equal positioning of all the cement samples. With increasing time, there is a complete absence of a gap between bone and implant in all doped samples except in pure BrC samples, where a shadow of the radiolucent zone was still visible. This is due to the initiation of bone formation from the host bone, which was more prominent for Sr-BrC and Sr+Mg-BrC. Enhanced bone formation for doped cement samples at early stages strongly supports our hypothesis that *in vivo* conditions, the overall bone regeneration can be enhanced by metal ion doping in BrC. The enhanced bone formation is also confirmed by fluorochrome labeling. When observed under UV light, the labeled new bone and old bone emit bright golden-yellow and dark-sea green fluorescence, which provides practical information in assessing the amount of new bone formation and bone healing [46]. Higher golden yellow fluorescence is noticed for Sr-BrC, Mg-BrC, and Sr+Mg-BrC cement samples. This is due to the significant effects of a single individual or binary dopants, which may help cellular proliferation and osteoblastic activity. Effects of Sr and Mg on cellular activity have also been studied in bone replacement materials such as bioglass, hydroxyapatite, and β -tricalcium phosphate systems [21,47]. It has been shown that 1wt% Sr and Mg can significantly enhance osteoblast proliferation and differentiation [21,22,30].

Owing to the high solubility, BrC rapidly degrades by chemical dissolution and cellular activity *in vivo*. It has been reported that BrC can degrade almost 70% in serum media

in vitro [48]. Dissolution of doped BrC releases Sr and Mg ions from the doped BrC to the region of new bone formation. In similar BrC formulations, it has been reported that nearly 15 parts per million (ppm) Sr²⁺ are released in the surrounding media *in vitro* [16]. Sr²⁺ is known to play a critical role in overall bone turnover. Early differentiation of osteoblast cells has been associated with Sr²⁺, which helps in the early expression of *cbfa 1* gene, essential for osteoblast differentiation [49]. Sr's presence can also stimulate the calcium-sensing receptor and other equivalent signaling pathways to induce early osteoblast differentiation [29]. Histological evaluation at the bone-implant interface confirms higher osteoblastic activity at 2 months in Sr-BrC cement. Similarly, Mg also plays a vital role in bone remodeling. Osteoblastic activity Mg-BrC cement may be due to Mg dopants' effect, which acts as a substitute for Ca in transport and mineralization processes, apart from its actions like enzyme co-factor function modulation of the action of hormones, growth factors, and cytokines. Furthermore, Mg-containing brushite-forming cement may facilitate the osteoblast cells to proliferate and express the differentiation marker of alkaline phosphatase (ALP) [11,50]. Higher osteoblastic activity and lamellar bone formation are prominent in binary Sr+Mg doped BrC due to the combining effects of both dopants on the bone formation processes of resorption and mineral aggregation. In general, woven bone is replaced by lamellar bone as growth and remodeling continue, corroborating the findings in binary-doped samples [51].

Bone remodeling and integration with bone cement is a continuous and dynamic process controlled by several factors, including osteoblastic synthesis and osteoclastic degradation of the bone matrix. Sr and Mg ions' presence has been critical in controlling the bone regeneration process. With time, the degradation of BrC releases Sr and Mg ions in the bone-implant interface. Higher osseointegration of the doped BrC at 4 months can be explained in many ways. It has been reported that Mg can slow down osteoclast formation, proliferation, and chemotaxis, increasing bone growth [18–20,52,53]. Moreover, the presence of Mg can significantly overexpress β_1 , $\alpha_5\beta_1$, and $\alpha_3\beta_1$ integrin, collagen type 1, essential signaling proteins, such as Shc (Src homology collagen), focal adhesion kinase that are essential for osteoblast activity [44–56]. Similarly, Sr controls key proteolytic enzymes, matrix metalloproteinase-2 (MMP-2) and matrix metalloproteinase-9 (MMP-9), along with osteoprotegerin (OPG) and receptor activator of nuclear factor κ - β ligand (RANKL) that is produced by osteoblast cells and are critical signaling mechanisms of osteoclast formation and its resorptive activity [19,20,57,58]. In a combined effect of reduced osteoclastic resorption and enhanced osteoblastic activity due to the presence of Sr, the overall bone formation enhances. The cellular activity around the implant sites indicates that fibroblastic activity is transformed into osteoblastic activity for all 4 cement samples. Still, higher osteoblastic activity and lamellar bone formation are observed in 1wt% Sr+ 1wt% Mg-BrC cement samples. Higher osteoblastic activity and lamellar bone formation are prominent in binary Sr+Mg doped BrC due to the combined effects of both dopants on the bone formation processes of resorption and mineral aggregation.

The enhanced bone formation for doped samples, as indicated by radiographic images where it is impossible to differentiate the host and the new bone and fluorochrome labeling, is due to the presence of Sr and Mg in the BrC. In a study involving three different types of cement, a similar observation of an initial radiolucent zone followed by gradual absence and almost

equal radiodensity to the adjacent bone was noticed in most of the 6 month samples [5]. In general, woven bone is eventually replaced by lamellar bone as growth and remodeling continue, corroborating the findings in binary-doped samples.

5.0 Conclusions

In this study, we have evaluated the effects of low-dose Sr and Mg addition on the *in vivo* biocompatibility of brushite cement (BrC) in a rabbit tibia model over 4 months. The effect of 1wt% Sr and 1wt% Mg doping was evident in better osseointegration, as indicated by a reduction in radiolucent zones at the defect site. Oxytetracycline fluorochrome labeling also confirmed higher bone deposition for doped samples. Moreover, higher osteoblastic activity was noticed around the Sr and Sr+Mg doped BrC. Overall, it can be concluded that a combination of Sr and Mg binary doping can effectively modulate the osseointegration of BrC and bone remodeling around the defect site, a much-needed property in bone replacement materials.

Acknowledgments

The authors would like to acknowledge financial support from the National Institutes of Health, NIBIB (Grant # R01 EB-007351), and NIDCR (Grant # R01 DE029204). The content is solely the authors' responsibility and does not necessarily represent the National Institutes of Health's official views. The authors wish to acknowledge the Vice-Chancellor, West Bengal University of Animal and Fishery Sciences, Kolkata, India, for his generous and kind support of this work. The authors would also like to acknowledge *in vivo* image quantification support from Mr. Arjak Bhattacharjee of Washington State University.

8.0 Data availability statement

Any additional data will be available upon request.

9.0 References

- [1]. Bohner M, Gbureck U, Barralet JE. Technological issues for the development of more efficient calcium phosphate bone cements: A critical assessment. *Biomaterials* 2005;26:6423–6429. doi:10.1016/j.biomaterials.2005.03.049 [PubMed: 15964620]
- [2]. Hurlle K, Oliveira JM, Reis RL, Pina S, Goetz-Neunhoffer F, “Ion-doped Brushite Cements for Bone Regeneration,” *Acta Biomater*, 123, pp. 51–71 (2021). [PubMed: 33454382]
- [3]. Tamimi F, Sheikh Z, Barralet J. Dicalcium phosphate cements: Brushite and monetite. *Acta Biomaterialia* 2012;8:474–487. doi:10.1016/j.actbio.2011.08.005
- [4]. Ginebra MP, Espanol M, Montufar EB, Perez RA, Mestres G. New processing approaches in calcium phosphate cements and their applications in regenerative medicine. *Acta Biomaterialia* 2010;6:2863–2873. doi:10.1016/j.actbio.2010.01.036
- [5]. Apelt D, Theiss F, El-Warrak AO, Zlinszky K, Bettschart-Wolfisberger R, Bohner M, et al. *In vivo* behavior of three different injectable hydraulic calcium phosphate cements. *Biomaterials* 2004;25:1439–1451. doi:10.1016/j.biomaterials.2003.08.073 [PubMed: 14643619]
- [6]. Tamimi F, Torres J, Lopez-Cabarcos E, Bassett DC, Habibovic P, Luceron E, et al. Minimally invasive maxillofacial vertical bone augmentation using brushite based cements. *Biomaterials* 2009;30:208–216. doi:10.1016/j.biomaterials.2008.09.032 [PubMed: 18845335]
- [7]. Pina S, Ferreira JMF. Brushite-Forming Mg-, Zn- and Sr-Substituted Bone Cements for Clinical Applications. *Materials* 2010;3:519–535. doi:10.3390/ma3010519
- [8]. Bohner M. Reactivity of calcium phosphate cements. *Journal of Materials Chemistry* 2007;17:3980. doi:10.1039/b706411j

- [9]. Pina S, Vieira SI, Rego P, Torres PMC, Da Cruz e Silva OAB, Da Cruz e Silva EF, et al. Biological responses of brushite-forming Zn- and ZnSr- substituted beta-tricalcium phosphate bone cements. *Eur Cell Mater* 2010;20:162–177. [PubMed: 20821372]
- [10]. Pina S, Vieira SI, Torres PMC, Goetz-Neunhoeffler F, Neubauer J, Da Cruz e Silva O a. B, et al. In vitro performance assessment of new brushite-forming Zn- and ZnSr-substituted β -TCP bone cements. *Journal of Biomedical Materials Research Part B: Applied Biomaterials* 2010;94B:414–420. doi:10.1002/jbm.b.31669
- [11]. Klammert U, Reuther T, Blank M, Reske I, Barralet JE, Grover LM, et al. Phase composition, mechanical performance and in vitro biocompatibility of hydraulic setting calcium magnesium phosphate cement. *ActaBiomaterialia* 2010;6:1529–1535. doi:10.1016/j.actbio.2009.10.021
- [12]. Bose S, Roy M, Bandyopadhyay A. Recent advances in bone tissue engineering scaffolds. *Trends Biotechnol.* 2012;30:546–554. doi:10.1016/j.tibtech.2012.07.005 [PubMed: 22939815]
- [13]. Patel ZS, Yamamoto M, Ueda H, Tabata Y, Mikos AG. Biodegradable gelatin microparticles as delivery systems for the controlled release of bone morphogenetic protein-2. *ActaBiomaterialia* 2008;4:1126–1138. doi:10.1016/j.actbio.2008.04.002
- [14]. Bose S, Tarafder S. Calcium phosphate ceramic systems in growth factor and drug delivery for bone tissue engineering: A review. *ActaBiomaterialia* 2012;8:1401–1421. doi:10.1016/j.actbio.2011.11.017
- [15]. Alkhraisat MH, Mariño FT, Rodríguez CR, Jerez LB, Cabarcos EL. Combined effect of strontium and pyrophosphate on the properties of brushite cements. *ActaBiomaterialia* 2008;4:664–670. doi:10.1016/j.actbio.2007.12.001
- [16]. Alkhraisat MH, Moseke C, Blanco L, Barralet JE, Lopez-Carbacos E, Gbureck U. Strontium modified bioceramics with zero order release kinetics. *Biomaterials* 2008;29:4691–4697. doi:10.1016/j.biomaterials.2008.08.026 [PubMed: 18804862]
- [17]. Lilley KJ, Gbureck U, Knowles JC, Farrar DF, Barralet JE. Cement from magnesium substituted hydroxyapatite. *Journal of Materials Science: Materials in Medicine* 2005;16:455–460. doi:10.1007/s10856-005-6986-3 [PubMed: 15875256]
- [18]. Bose S, Tarafder S, Bandyopadhyay A, “Effect of Chemistry on Osteogenesis and Angiogenesis Towards Bone Tissue Engineering Using 3D Printed Scaffolds,” *Annals of Biomedical Engineering*, 45 (1), pp. 261–272 (2017). [PubMed: 27287311]
- [19]. Ke D, Tarafder S, Vahabzadeh S, Bose S, “Effects of MgO, ZnO, SrO, and SiO₂ in tricalcium phosphate scaffolds on *in vitro* genes expression and *in vivo* osteogenesis,” *Materials Science and Engineering: C* 96, pp. 10–19 (2019). [PubMed: 30606515]
- [20]. Fielding G, Smoot W. and Bose S. “Effects of SiO₂, SrO, MgO and ZnO dopants in TCP on osteoblastic Runx2 expression,” *Journal of Biomedical Materials Research Part A*, 102(7):2417–26 (2014). doi: 10.1002/jbm.a.34909. [PubMed: 23946240]
- [21]. Bandyopadhyay A, Bernard S, Xue W, Bose S. Calcium Phosphate-Based Resorbable Ceramics: Influence of MgO, ZnO, and SiO₂ Dopants. *Journal of the American Ceramic Society* 2006;89:2675–2688. doi:10.1111/j.1551-2916.2006.01207.x
- [22]. Banerjee SS, Tarafder S, Davies NM, Bandyopadhyay A, Bose S. Understanding the influence of MgO and SrO binary doping on the mechanical and biological properties of β -TCP ceramics. *ActaBiomaterialia* 2010;6:4167–4174. doi:10.1016/j.actbio.2010.05.012
- [23]. Bose S, Tarafder S, Banerjee SS, Davies NM, Bandyopadhyay A. Understanding in vivo response and mechanical property variation in MgO, SrO and SiO₂ doped β -TCP. *Bone* 2011;48:1282–1290. doi:10.1016/j.bone.2011.03.685 [PubMed: 21419884]
- [24]. Fadeev IV, Shvorneva LI, Barinov SM, Orlovskii VP. Synthesis and Structure of Magnesium-Substituted Hydroxyapatite. *Inorganic Materials* 2003;39:947–950. doi:10.1023/A:1025509305805
- [25]. Suchanek WL, Byrappa K, Shuk P, Riman RE, Janas VF, TenHuisen KS. Mechanochemical-hydrothermal synthesis of calcium phosphate powders with coupled magnesium and carbonate substitution. *Journal of Solid State Chemistry* 2004;177:793–799. doi:10.1016/j.jssc.2003.09.012
- [26]. Vahabzadeh S, Robertson S, Bose S, “Beta-phase stabilization and increased osteogenic differentiation of stem cells by solid-state synthesized magnesium tricalcium phosphate,” *Journal of Materials Research*, 36 (15), pp. 3041–3049 (2021). [PubMed: 35757291]

- [27]. Tarafder S, Dernel W, Bandyopadhyay A and Bose S, “SrO and MgO doped microwave sintered 3D printed tricalcium phosphate scaffolds: Mechanical properties and *in vivo* osteogenesis in a rabbit model,” *Journal of Biomedical Materials Research- Applied Biomaterials*, 103 (3), (2015). DOI: 10.1002/jbm.b.33239
- [28]. Baron R, Tsouderos Y. In vitro effects of S12911–2 on osteoclast function and bone marrow macrophage differentiation. *European Journal of Pharmacology* 2002;450:11–17. doi:10.1016/S0014-2999(02)02040-X [PubMed: 12176103]
- [29]. Marie PJ. Strontium ranelate: a novel mode of action optimizing bone formation and resorption. *Osteoporosis International* 2005;16:S7–S10. doi:10.1007/s00198-004-1753-8 [PubMed: 15578159]
- [30]. Roy M, Bandyopadhyay A, Bose S. Induction plasma sprayed Sr and Mg doped nano hydroxyapatite coatings on Ti for bone implant. *Journal of Biomedical Materials Research Part B: Applied Biomaterials* 2011;99B:258–265. doi:10.1002/jbm.b.31893
- [31]. Fang J, Dong W, Peng H, Xu Y, Jia W, Liang L, Liang Y., Study on reconstruction of rabbit alveolar bone defect with strontium-containing brushite bone cements, *The Journal of Practical Medicine* 34 (5) (2018) 720–724.
- [32]. Taha A, Akram M, Jawad Z, Alshemary AZ, Hussain R, Strontium doped injectable bone cement for potential drug delivery applications. *Materials science & engineering C, Materials for biological applications* 80 (2017) 93–101. [PubMed: 28866230]
- [33]. <https://americanbonehealth.org/medications-bone-health/why-strontium-is-not-advised-for-bone-health/> (Accessed on May 19, 2022).
- [34]. Alkhraisat MH, Cabrejos-Azama J, Rodríguez CR, Jerez LB, Cabarcos EL., Magnesium substitution in brushite cements, *Materials science & engineering C, Materials for biological applications* 33 (2013) 475–481. [PubMed: 25428098]
- [35]. Saleh AT, Ling LS, Hussain R., Injectable magnesium-doped brushite cement for controlled drug release application, *Journal of Materials Science* 51 (2016) 7427–7439.
- [36]. Cabrejos-Azama J, Alkhraisat MH, Rueda C, Torres J, Pintado C, Blanco L, López-Cabarcos E. Magnesium substitution in brushite cements: Efficacy of a new biomaterial loaded with vancomycin for the treatment of *Staphylococcus aureus* infections. *Materials science & engineering C, Materials for biological applications* 61 (2016) 72–78. [PubMed: 26838826]
- [37]. Han B, Ma P-W, Zhang L-L, Yin Y-J, Yao K-D, Zhang F-J, et al. β -TCP/MCPM-based premixed calcium phosphate cements. *Acta Biomaterialia* 2009;5:3165–3177. doi:10.1016/j.actbio.2009.04.024
- [38]. Roy M, DeVoe K, Bandyopadhyay A, Bose S. Mechanical property and in vitro biocompatibility of brushite cement modified by polyethylene glycol. *Materials Science and Engineering: C n.d.* doi:10.1016/j.msec.2012.05.020
- [39]. Bohner M, Lemaitre J, Ring TA. Effects of Sulfate, Pyrophosphate, and Citrate Ions on the Physicochemical Properties of Cements Made of β -Tricalcium Phosphate-Phosphoric Acid-Water Mixtures. *Journal of the American Ceramic Society* 1996;79:1427–1434. doi:10.1111/j.1151-2916.1996.tb08746.x
- [40]. Dey A, Nandi SK, Kundu B, Kumar C, Mukherjee P, Roy S, et al. Evaluation of hydroxyapatite and β -tri calcium phosphate microplasma spray coated pin intra-medullary for bone repair in a rabbit model. *Ceramics International* 2011;37:1377–1391. doi:10.1016/j.ceramint.2011.01.005
- [41]. Sarkar K, Kumar V, Bavya Devi K., Ghosh D, Nandi SK, and Roy M, Anomalous in Vitro and in Vivo Degradation of Magnesium Phosphate Bioceramics: Role of Zinc Addition, *ACS Biomaterials Science & Engineering* 2019 5(10), 5097–5106. DOI: 10.1021/acsbiomaterials.9b00422 [PubMed: 33455257]
- [42]. Bohner M, Van Landuyt P, Merkle HP, Lemaitre J. Composition effects on the pH of a hydraulic calcium phosphate cement. *J Mater Sci Mater Med* 1997;8:675–681. [PubMed: 15348818]
- [43]. Nurit J, Margerit J, Terol A, Boudeville P. pH-metric study of the setting reaction of monocalcium phosphate monohydrate/calcium oxide-based cements. *J Mater Sci Mater Med* 2002;13:1007–1014. [PubMed: 15348169]

- [44]. Arinzech TL, Peter SJ, Archambault MP, Van den Bos C, Gordon S, Kraus K, et al. Allogeneic mesenchymal stem cells regenerate bone in a critical-sized canine segmental defect. *J Bone Joint Surg Am* 2003;85-A:1927–1935. [PubMed: 14563800]
- [45]. Kundu B, Nandi S, Dasgupta S, Datta S, Mukherjee P, Roy S, et al. Macro-to-micro porous special bioactive glass and ceftriaxone–sulbactam composite drug delivery system for treatment of chronic osteomyelitis: an investigation through in vitro and in vivo animal trial. *Journal of Materials Science: Materials in Medicine* 2011;22:705–720. doi:10.1007/s10856-010-4221-3 [PubMed: 21221731]
- [46]. Nandi SK, Ghosh SK, Kundu B, De DK, Basu D. Evaluation of new porous β -tri-calcium phosphate ceramic as bone substitute in goat model. *Small Ruminant Research* 2008;75:144–153. doi:10.1016/j.smallrumres.2007.09.006
- [47]. Hoppe A, Güldal NS, Boccaccini AR. A review of the biological response to ionic dissolution products from bioactive glasses and glass-ceramics. *Biomaterials* 2011;32:2757–2774. doi:10.1016/j.biomaterials.2011.01.004 [PubMed: 21292319]
- [48]. Grover LM, Knowles JC, Fleming GJP, Barralet JE. In vitro ageing of brushite calcium phosphate cement. *Biomaterials* 2003;24:4133–4141. doi:10.1016/S0142-9612(03)00293-X [PubMed: 12853243]
- [49]. Sila-Asna M, Bunyaratvej A, Maeda S, Kitaguchi H, Bunyaratavej N. Osteoblast differentiation and bone formation gene expression in strontium-inducing bone marrow mesenchymal stem cell. *Kobe J Med Sci* 2007;53:25–35. [PubMed: 17579299]
- [50]. Nadler MJ, Hermosura MC, Inabe K, Perraud AL, Zhu Q, Stokes AJ, et al. LTRPC7 is a Mg²⁺-ATP-regulated divalent cation channel required for cell viability. *Nature* 2001;411:590–595. doi:10.1038/35079092 [PubMed: 11385574]
- [51]. Currey J. The many adaptations of bone. *Journal of Biomechanics* 2003;36:1487–1495. doi:10.1016/S0021-9290(03)00124-6 [PubMed: 14499297]
- [52]. Janning C, Willbold E, Vogt C, Nellesen J, Meyer-Lindenberg A, Windhagen H, et al. Magnesium hydroxide temporarily enhancing osteoblast activity and decreasing the osteoclast number in peri-implant bone remodelling. *Acta Biomaterialia* 2010;6:1861–1868. doi:10.1016/j.actbio.2009.12.037
- [53]. Roy M, Bose S. Osteoclastogenesis and osteoclastic resorption of tricalcium phosphate: Effect of strontium and magnesium doping. *Journal of Biomedical Materials Research Part A* 2012;n/a–n/a. doi:10.1002/jbm.a.34181
- [54]. Zreiqat H, Howlett CR, Zannettino A, Evans P, Schulze-Tanzil G, Knabe C, et al. Mechanisms of magnesium-stimulated adhesion of osteoblastic cells to commonly used orthopaedic implants. *Journal of Biomedical Materials Research* 2002;62:175–184. doi:10.1002/jbm.10270 [PubMed: 12209937]
- [55]. Gronthos S, Stewart K, Graves SE, Hay S, Simmons PJ. Integrin Expression and Function on Human Osteoblast-like Cells. *Journal of Bone and Mineral Research* 1997;12:1189–1197. doi:10.1359/jbmr.1997.12.8.1189 [PubMed: 9258748]
- [56]. Schlaepfer DD, Hanks SK, Hunter T, Geer van der P. Integrin-mediated signal transduction linked to Ras pathway by GRB2 binding to focal adhesion kinase. Published online: 29 December 1994; | doi:10.1038/372786a0 1994;372:786–791. doi:10.1038/372786a0
- [57]. Tat SK, Pelletier J-P, Mineau F, Caron J, Martel-Pelletier J. Strontium ranelate inhibits key factors affecting bone remodeling in human osteoarthritic subchondral bone osteoblasts. *Bone* 2011;49:559–567. doi:10.1016/j.bone.2011.06.005 [PubMed: 21700005]
- [58]. Boyle WJ, Simonet WS, Lacey DL. Osteoclast differentiation and activation. *Nature* 2003;423:337–342. doi:10.1038/nature01658 [PubMed: 12748652]

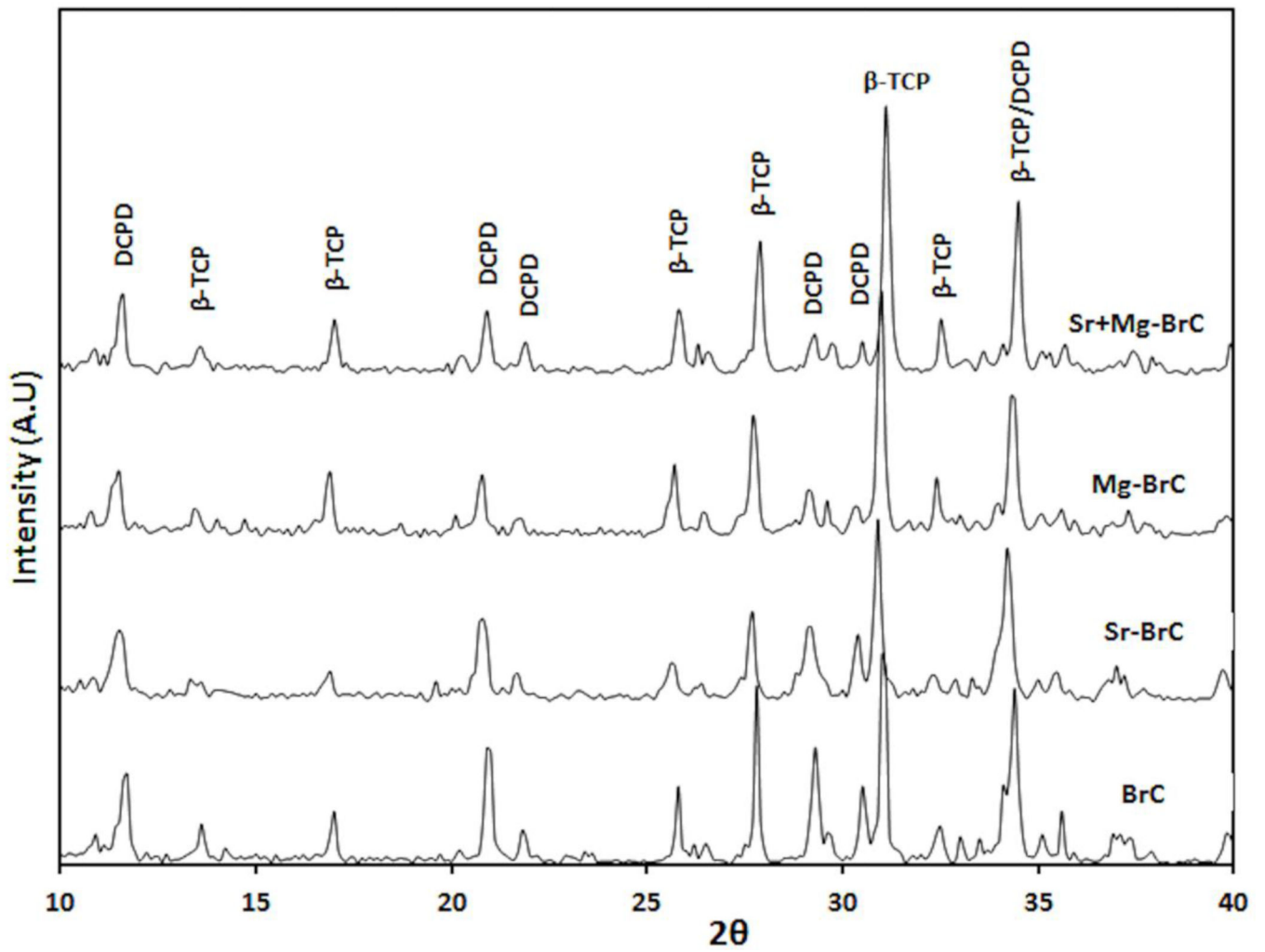


Fig. 1:
XRD results of pure and doped BrC cement incubated in PBS for 1 day.

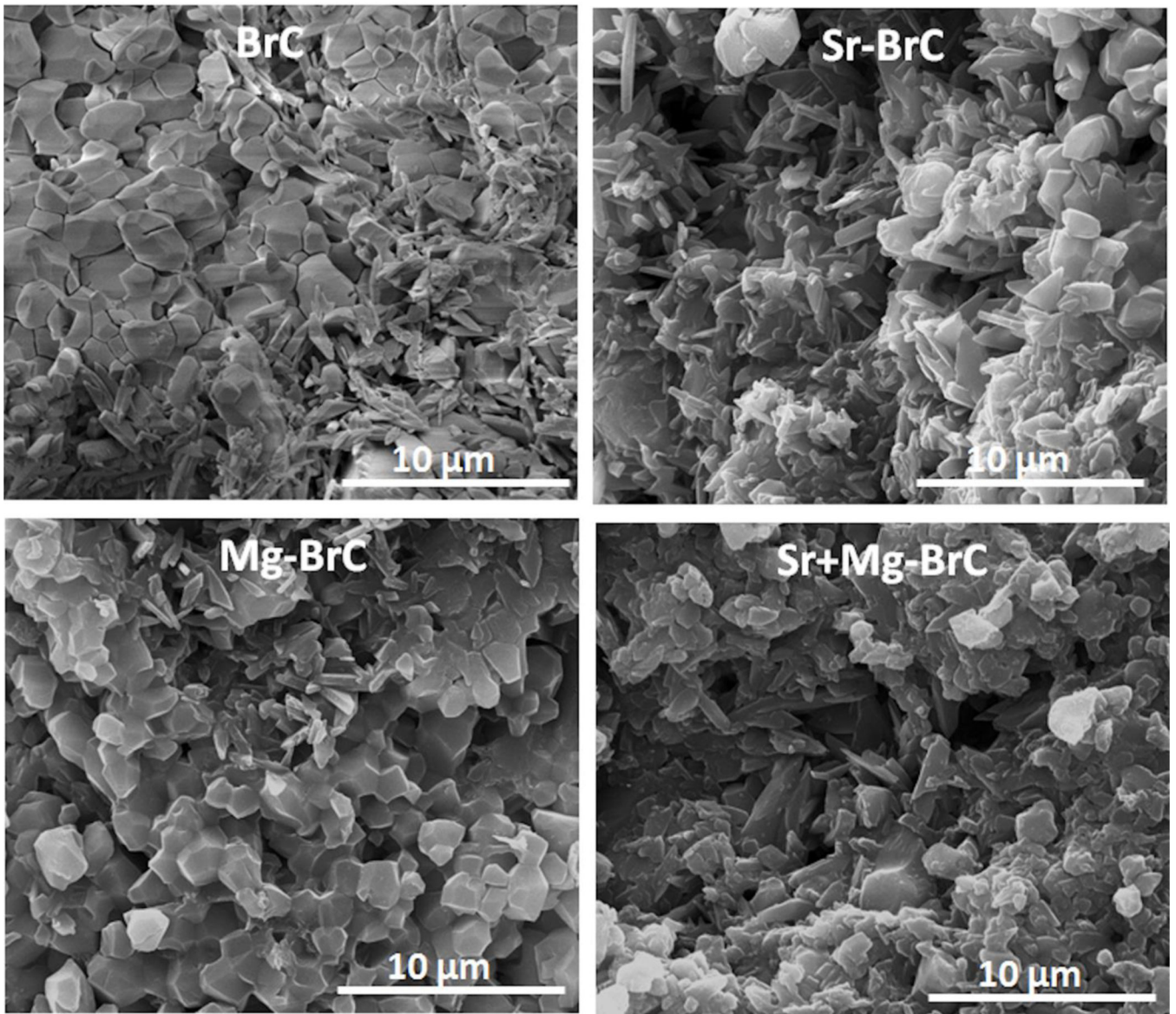


Fig. 2:
FESEM micrographs of four different cement samples after incubation in PBS for day 1.

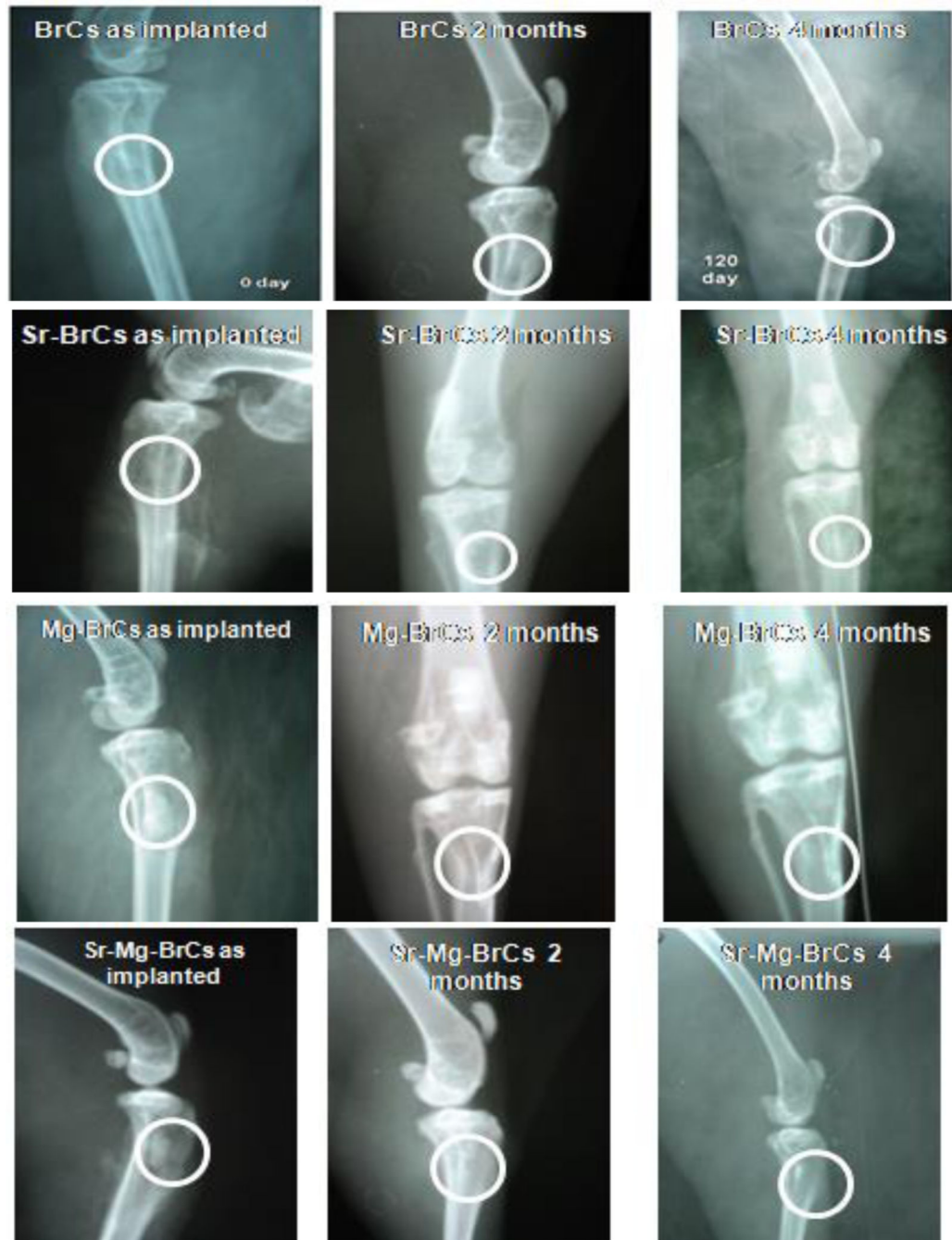


Fig. 3:
X-ray images depicting cement implanted in the proximal tibia over 4 months (Round zone is an area of implantation and subsequent bone formation)

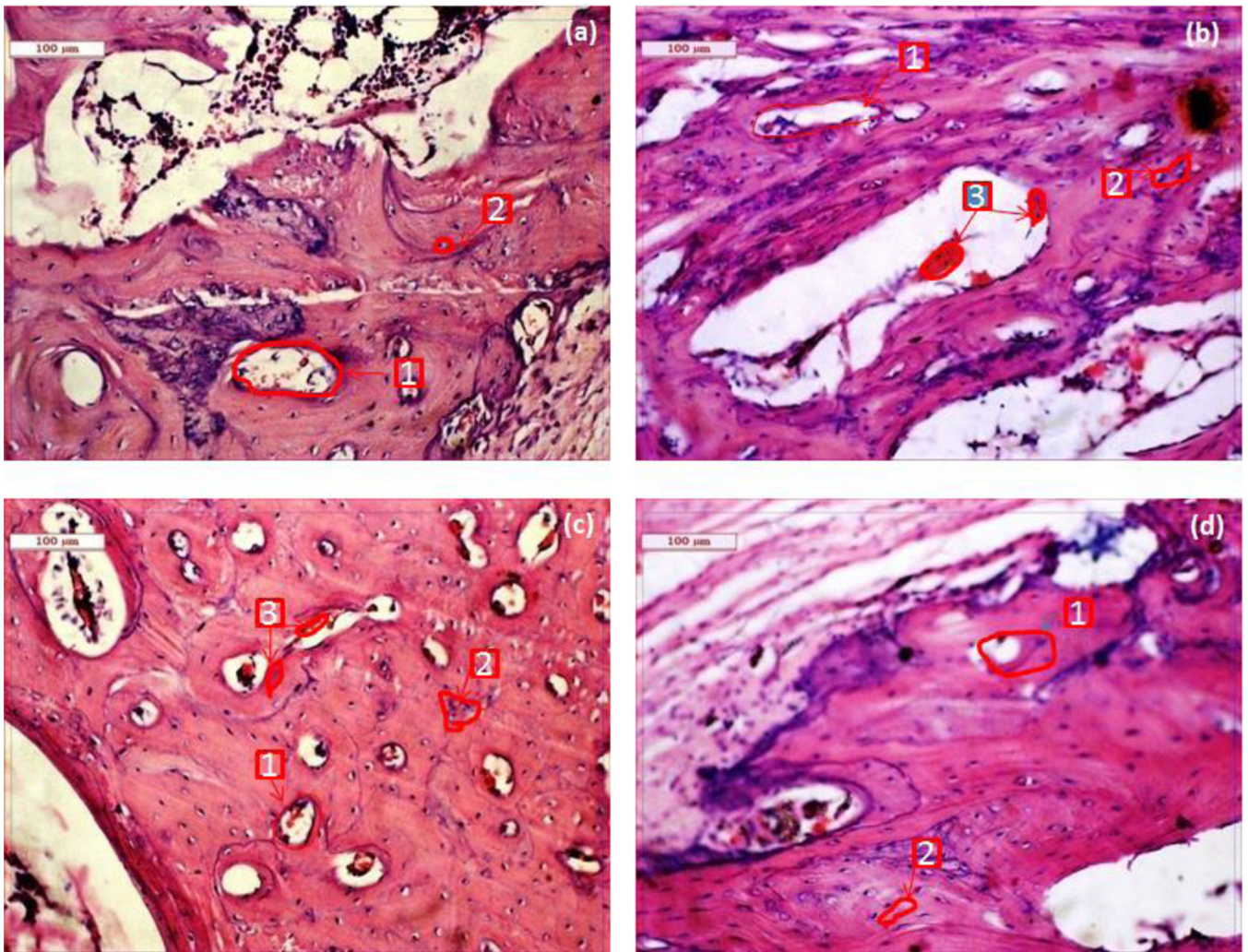


Fig. 4: Histological images depicting cement implanted bone at 2 months (a) BrC cement, (b) Sr-BrC cement, (c) Mg-BrC cement, and (d) Sr+Mg-BrC cement indicating haversian canal (1), osteoblast (2), angiogenesis (3).

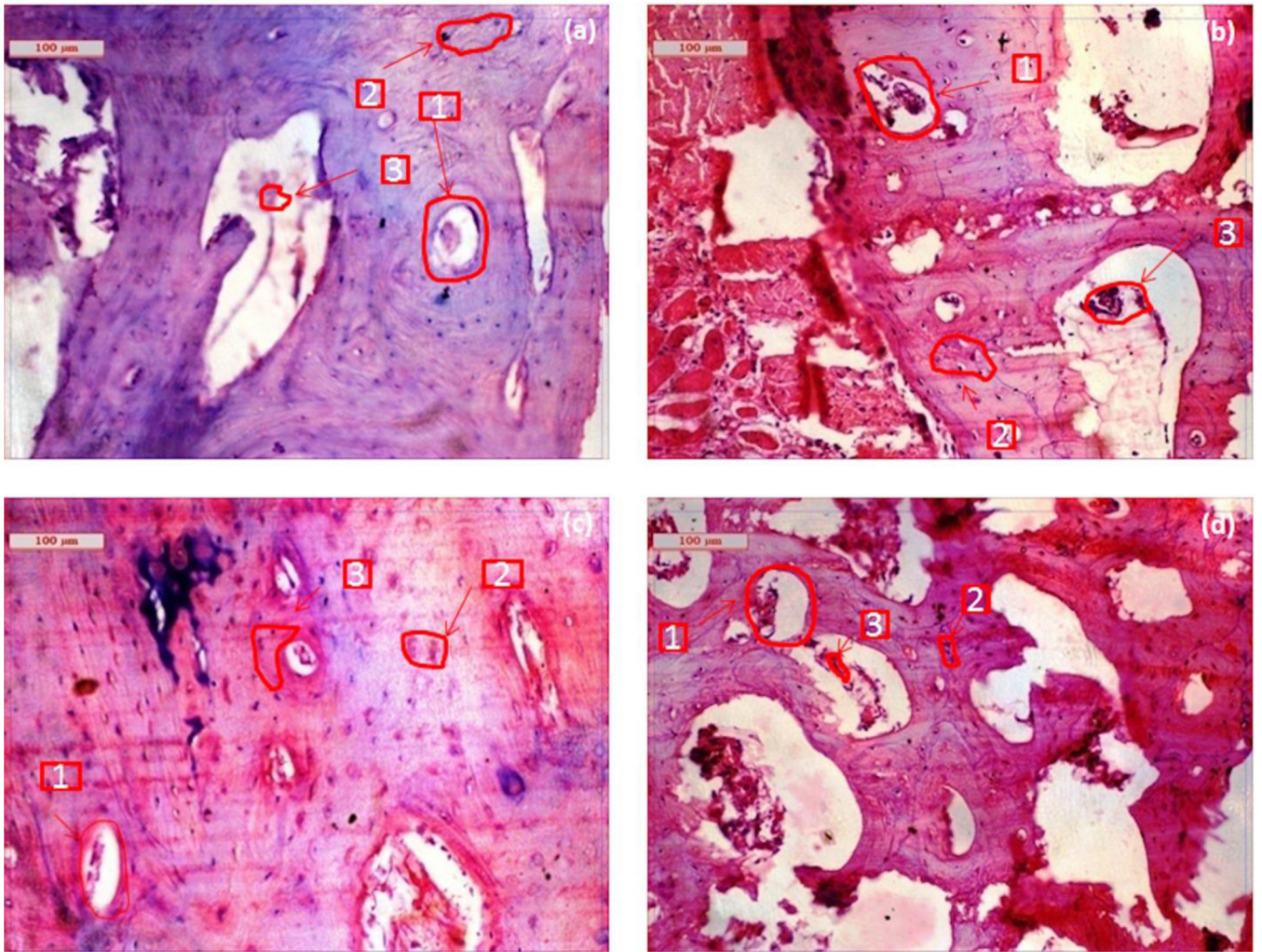
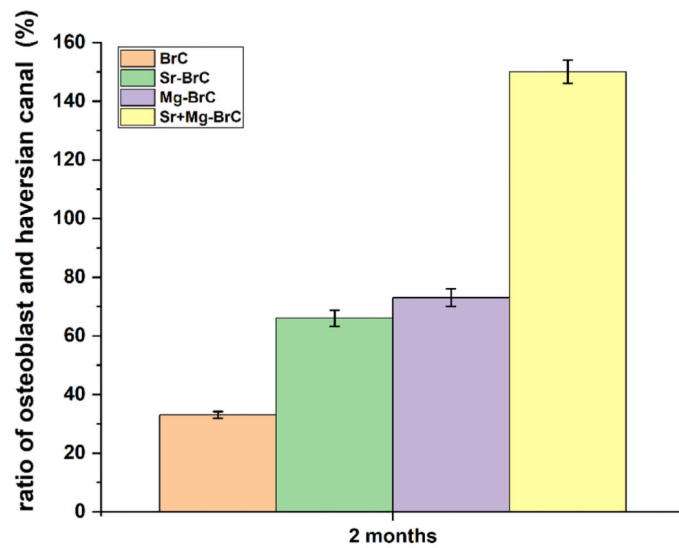
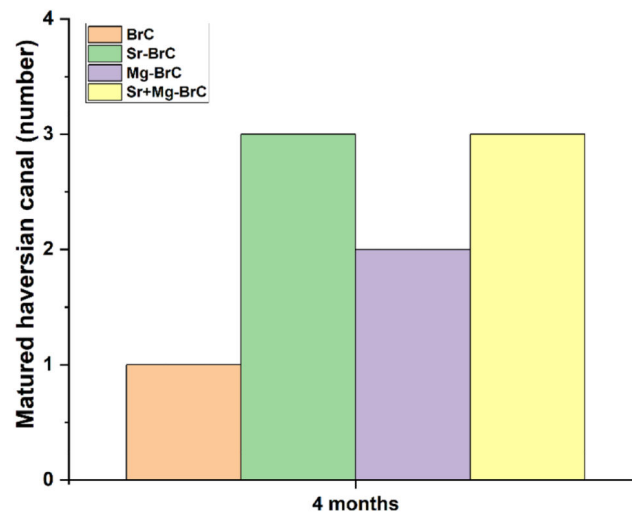


Fig. 5: Histological images depicting cement implanted bone at 4 months (a) BrC cement, (b) Sr-BrC cement, (c) Mg-BrC cement, and (d) Sr+Mg-BrC cement indicating Haversian canal (1), osteoblast (2), angiogenesis (3).



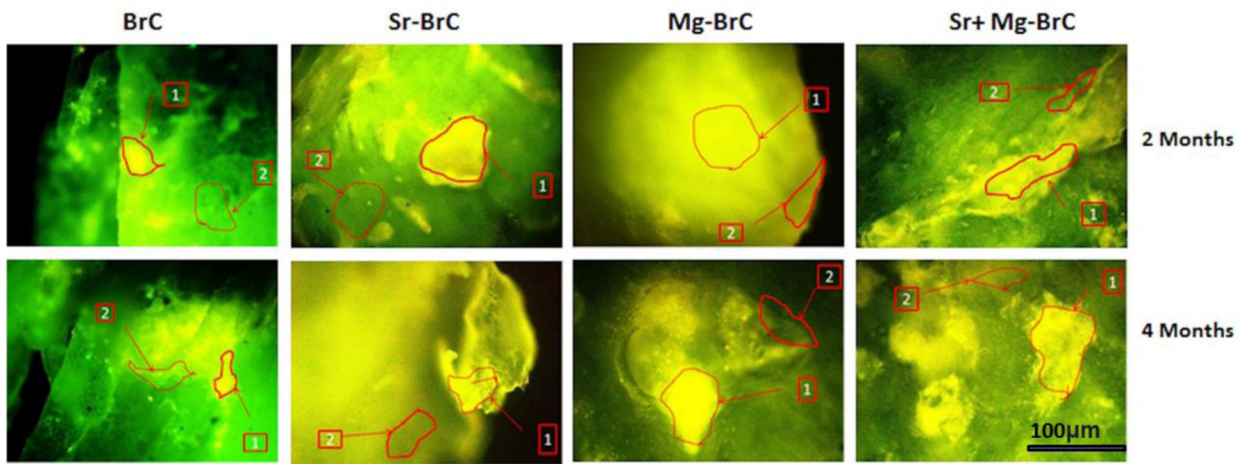
(a)



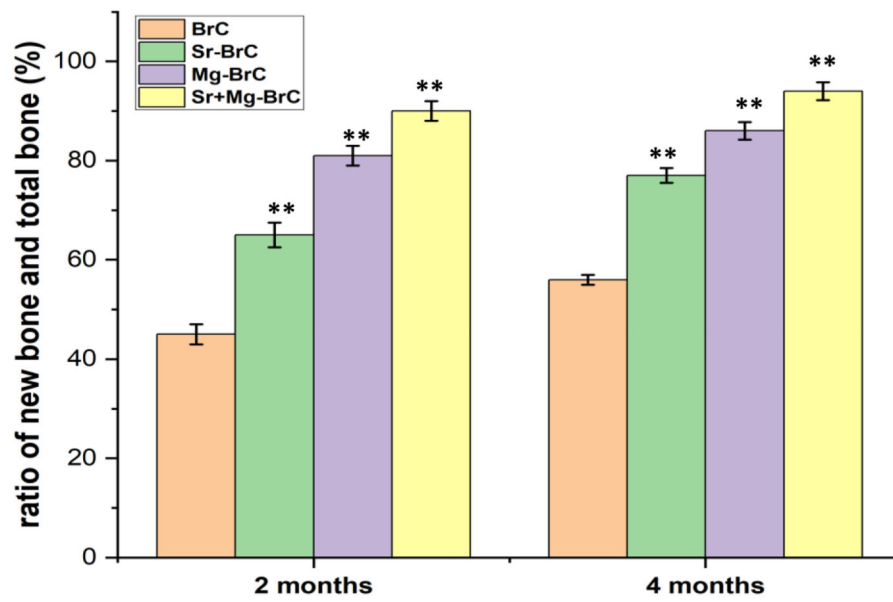
(b)

Fig. 6:

(a) The ratio of osteoblast and Haversian canal (%) after 2 months of implantation. All treatment samples show a significantly higher ratio than control (** denotes $p < 0.0001$). (b) The number of matured Haversian canals in each sample. Treatments show a higher number of canals than the control.



(a)



(b)

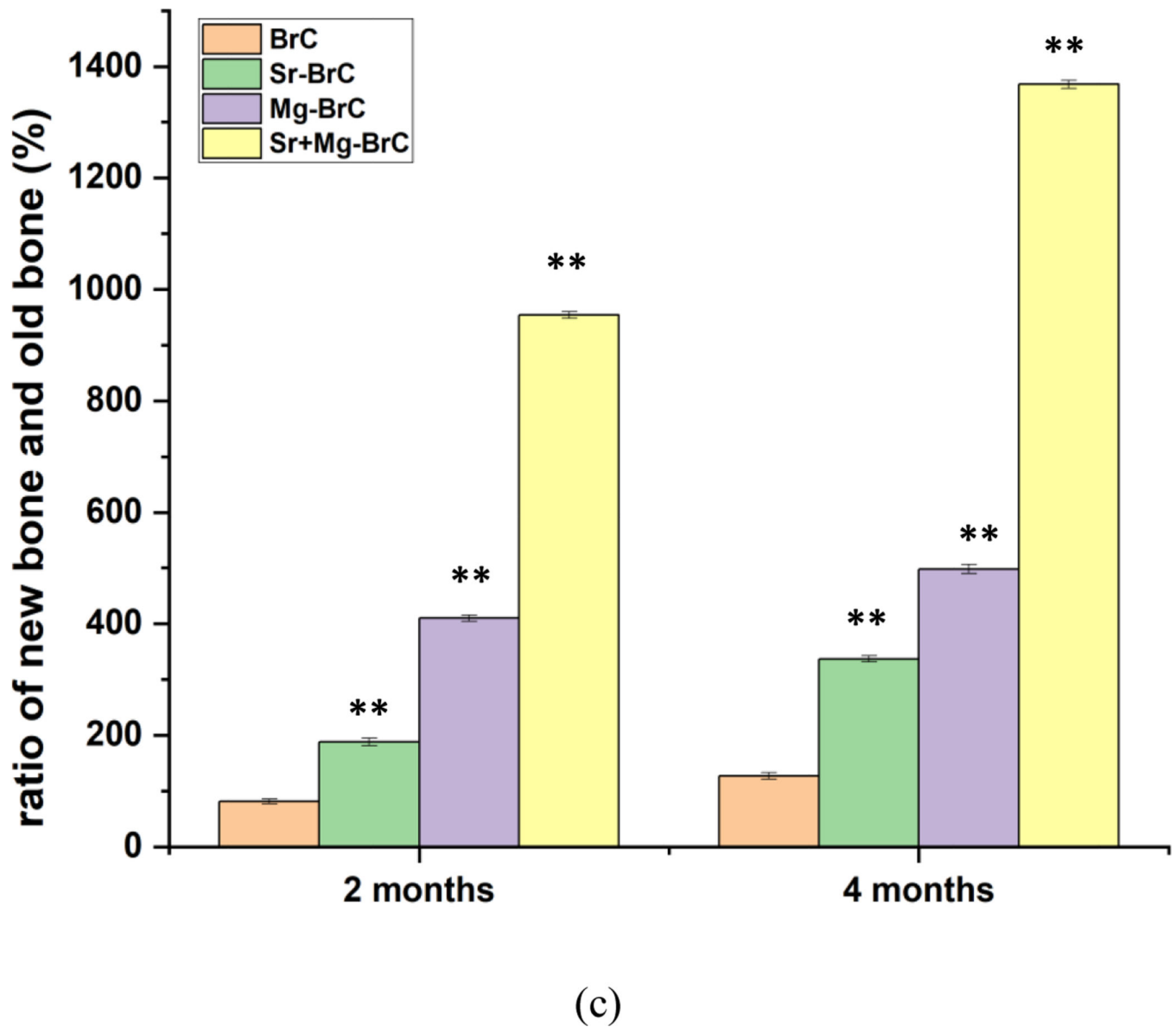


Fig. 7:

(a) Fluorochrome labeling images depicted bone formation in 2 and 4 months for the pure and doped BrC cement. (1) Golden yellow fluorescence- new bone (2) Sea green fluorescence- old bone. (b) The ratio of new bone formation with total bone (c) the ratio of new bone formation with old bone, as calculated from the ImageJ software. The statistical data analysis shows a significant difference between the treatment and control. (** denotes $p < 0.0001$)

Table 1:

Properties of pure and doped brushite cement.

Sample	Composition	Initial Set Time (min)	Final Set Time (min)	Brushite	β -TCP
BrC	BrC	4	9	27	73
Sr-BrC	BrC+1.0 w % SrO	4	8	43	57
Mg-BrC	BrC+1.0 w % MgO	6	15	31	69
Sr+Mg-BrC	BrC+1.0 w % SrO + 1.0 w % MgO	4	12	21	79

Author Manuscript

Author Manuscript

Author Manuscript

Author Manuscript